

Very Low Pressure Reactor Study of the  $\text{H} + \text{HBr} \rightleftharpoons \text{H}_2 + \text{Br}$  Reaction

Terence J. Mitchell, Alicia C. Gonzalez, and Sidney W. Benson\*

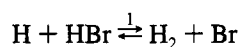
Donald P. and Katherine B. Loker Hydrocarbon Research Institute, University of Southern California, University Park, Los Angeles, California 90089-1661

Received: June 20, 1995; In Final Form: August 30, 1995<sup>⊗</sup>

The reaction of H atoms, generated by microwave discharge of  $\text{H}_2/\text{Ar}$  gas mixtures, with HBr has been studied employing the very low pressure reactor (VLPR) technique. Reactants and reaction products were followed by mass spectrometry. Rate constants of  $(5.4 \pm 0.7) \times 10^{-12}$ ,  $(6.3 \pm 0.8) \times 10^{-12}$ , and  $(6.8 \pm 0.4) \times 10^{-12} \text{ cm}^3 \text{ molecule}^{-1} \text{ s}^{-1}$  were extracted for the title reaction at 268, 298, and 333 K, respectively. Difficulties were encountered in obtaining mass balance closure for molecular hydrogen, owing to its production from the internal surfaces of the phosphoric acid coated quartz microwave tube. Formation of very small amounts of molecular bromine, detected at  $m/e$  158, 160, and 162, appeared due to some back-diffusion of HBr into the microwave tube.  $\text{Br}_2$  formation was observed to be a function of discharge power and, at sufficiently high powers, could be reduced below detection limits. Under these conditions, bromine mass balances ( $\text{Br}_2$ , Br, and HBr) were around  $(95 \pm 5)\%$ . A transition state calculation provides an estimated preexponential factor for the reaction in good agreement with our experimental results and with those available from the other most recent temperature-dependent studies. The temperature dependence of reaction 1 can be expressed by  $k_1/\text{cm}^3 \text{ molecule}^{-1} \text{ s}^{-1} = 9.96 \times 10^{-13} T^{0.5} \exp(-300/T)$  over the temperature range 200–1000 K.

## Introduction

The present study reports measurements of the rate constant for the reaction



using the very low pressure reactor (VLPR) technique over the temperature range 268–333 K. Several investigations of this reaction have previously been published in the literature,<sup>1–7</sup> with the two most recent having been reported during the course of the present study. The present work differs from the latter in that the reaction, initiated by microwave discharge through flowing  $\text{H}_2/\text{Ar}$  mixtures, has been studied at milli-Torr pressures, employing mass spectrometry (MS) to follow both reactants and products. Generally, the previously reported work has been conducted at pressures above 0.5 Torr using electron paramagnetic resonance (EPR),<sup>1,2,4</sup> resonance fluorescence (RF),<sup>3,6,7</sup> or resonance absorption (RA)<sup>5</sup> detection techniques. The present investigation of the title reaction evolved from a need to find a reaction with which to calibrate the absolute H atom concentration in our VLPR system. Reaction 1 appeared an ideal candidate. Some difficulty was, however, associated with applying this reaction to that purpose. The results of our study together with the difficulties encountered are discussed in detail.

## Experimental Section

Experiments were performed using the VLPR apparatus. The latter has been discussed in detail elsewhere,<sup>8</sup> and only a brief description, identifying differences from our previously employed system, is provided.

The gas-phase reaction occurs in a Knudsen cell at steady state and at pressures in the milli-Torr regime. Reactants, introduced through separate capillary inlets, undergo reaction

within the cell and subsequently, together with the products of reaction, flow out of the cell through an exit aperture. The molecular beam formed in the differentially pumped system is modulated prior to entering the ionizing field of a quadrupole mass spectrometer.

Gases employed were 5%  $\text{H}_2/\text{Ar}$  and 10%  $\text{HBr}/\text{Ar}$  mixtures. Argon and hydrogen mixtures (both Matheson Research Grade gases) were prepared in a 5 L storage bulb by prior direct measurement of the partial pressures of the components. Hydrogen bromide (Matheson Research Grade) was purified by repeated freeze–pump–thaw cycles at 77 K followed by bulb-to-bulb distillation under vacuum, prior to storage diluted in argon in a darkened 5 L bulb. Traces of water were removed by passing the gases through molecular sieves. Bromine, in a 2.5%  $\text{Br}_2/\text{Ar}$  mixture used for detection and calibration purposes, was purified, diluted, and stored in a manner similar to that detailed for HBr.

Reactant flows within the reactor were established *via* a flow subsystem by introducing gas mixtures from individual calibrated buffer volumes ( $\sim 500$  mL) through 100 cm long resistive capillaries. The internal diameters of the latter (0.020, 0.035, or 0.060 cm) could be varied to provide variations in flow rate. Upstream buffer pressures (8–40 Torr) used to establish the required flows were held constant throughout experiment to  $\pm 0.1$  Torr. Validyne DP 15-30 transducers were used to monitor gas pressures. Flow rates were calibrated in separate experiments by following the pressure drop across the chosen capillaries.

Hydrogen atoms were generated by flowing the  $\text{H}_2/\text{Ar}$  mixture through a quartz tube internally coated with phosphoric acid, enclosed within a 2.45-GHz microwave discharge cavity (KIVA Instruments Model MPG 4M microwave power generator) operated between 20 and 40 W. The  $\text{H}/\text{H}_2/\text{Ar}$  mixture passed from the microwave tube into the reactor through a tapered 0.1 cm capillary of 2 cm length with an apical opening diameter of 0.025 cm. To minimize back-flushing, the  $\text{HBr}/\text{Ar}$  mixture was admitted to the reaction cell *via* a  $0.1 \times 2.0$  cm capillary.

<sup>⊗</sup> Abstract published in *Advance ACS Abstracts*, October 15, 1995.

TABLE 1: Selected Experimental Data at T = 298 K

run no.	orif	[HBr] <sub>0</sub> /10 <sup>12</sup>	[HBr]/10 <sup>12</sup>	Δ[HBr]/[HBr] <sub>0</sub>	I <sub>H0</sub> /I <sub>H</sub>	k <sub>eH</sub> (I <sub>H0</sub> /I <sub>H</sub> - 1)	[H] <sub>ss</sub> /10 <sup>10</sup>	ΔF <sub>HBr</sub> /10 <sup>11</sup>	ΔF <sub>H2</sub> /10 <sup>12</sup>	ΔF <sub>H2</sub> /ΔF <sub>HBr</sub>	I <sub>Br</sub> /I <sub>HBr</sub>
1	φ <sub>2</sub>	5.32 <sup>a</sup>	0.41 <sup>a</sup>	92.3 <sup>b</sup>	1.45 <sup>c</sup>	2.18 <sup>d</sup>	100.0 <sup>e</sup>	26.4 <sup>e</sup>	4.40 <sup>e</sup>	1.67 <sup>f</sup>	0.97 <sup>c</sup>
2	φ <sub>2</sub>	5.35	0.41	92.3	1.42	2.00	100.0 <sup>g</sup>	26.4	3.64	1.38	0.87
5	φ <sub>2</sub>	1.72	1.39	19.1	2.85	8.87	2.0	1.76			
6	φ <sub>2</sub>	1.93	1.47	23.7	3.13	10.23	2.7	2.46			
10	φ <sub>2</sub>	2.38	1.94	18.5	3.63	12.60	1.9	2.32			
11	φ <sub>2</sub>	2.88	1.95	32.3	3.64	12.70	4.1	4.98	3.32	6.67	
14	φ <sub>2</sub>	2.88	2.25	21.8	4.14	15.08	2.4	3.34			
17	φ <sub>2</sub>	2.88	2.73	5.2	4.20	15.40	0.47	0.79			
18	φ <sub>2</sub>	3.43	2.86	16.5	4.63	17.50	1.7	3.04			
23	φ <sub>2</sub>	4.02	3.22	19.9	5.62	22.21	2.1	4.25			
24	φ <sub>2</sub>	5.35	3.60	32.7	6.23	25.20	4.1	9.38			
26	φ <sub>2</sub>	4.66	3.85	17.4	5.95	23.80	1.8	4.35			
28	φ <sub>2</sub>	5.35	4.18	21.9	6.76	27.68	2.4	6.24			
31	φ <sub>2</sub>	5.35	4.58	14.4	6.66	27.20	1.4	4.14	4.60	11.1	
32	φ <sub>2</sub>	5.35	4.75	11.2	6.79	27.90	1.1	3.21			
33	φ <sub>2</sub>	6.09	4.85	20.4	7.19	29.80	2.2	6.64			
35	φ <sub>2</sub>	6.87	5.74	16.4	9.82	42.40	1.7	6.08			
36	φ <sub>2</sub>	7.71	6.10	20.9	8.96	38.25	2.2	8.59			
37	φ <sub>2</sub>	6.88	6.23	9.4	9.18	39.30	0.89	3.47	5.07	14.6	0.74
38	φ <sub>2</sub>	5.35	2.71	49.3	5.07	18.62	8.3	14.1	2.12	1.5	0.95
39	φ <sub>2</sub>	5.35	2.77	48.3	4.87	19.56	8.0	13.8			0.97
3	φ <sub>3</sub>	0.95	0.80	16.2	1.81	8.03	3.4	1.71			
9	φ <sub>3</sub>	2.31	1.67	27.6	2.09	10.90	6.7	7.01			
15	φ <sub>3</sub>	2.65	2.36	10.8	2.56	15.50	2.1	3.12			
16	φ <sub>3</sub>	3.40	2.67	21.4	3.10	20.90	4.8	8.10			
19	φ <sub>3</sub>	3.01	2.92	3.0	2.75	17.30	0.55	1.05			
21	φ <sub>3</sub>	3.40	3.14	7.6	2.85	18.30	1.5	2.86			
22	φ <sub>3</sub>	4.70	3.19	32.2	2.53	15.20	8.4	16.8			
25	φ <sub>3</sub>	4.70	3.81	19.0	3.39	23.80	4.1	9.88			
29	φ <sub>3</sub>	5.19	4.49	13.4	3.54	25.30	2.7	7.74			
30	φ <sub>3</sub>	5.69	4.57	19.7	3.55	25.30	4.3	12.4			
34	φ <sub>3</sub>	7.35	5.42	26.3	3.96	29.40	6.3	21.3			
40	φ <sub>3</sub>	2.59	2.04	21.4	2.08	11.17	4.8	6.06	2.83	4.7	0.97
4	φ <sub>5</sub>	1.13	0.98	13.3	1.29	6.66	6.4	3.90			
7	φ <sub>5</sub>	2.00	1.55	22.5	1.39	9.02	12.0	11.6			
8	φ <sub>5</sub>	1.81	1.58	12.5	1.63	14.70	5.9	5.80			
12	φ <sub>5</sub>	2.42	2.16	10.8	1.67	15.50	5.0	6.87			
13	φ <sub>5</sub>	2.42	2.23	7.9	1.77	18.00	3.6	5.01			
20	φ <sub>5</sub>	3.13	2.93	6.3	1.91	21.20	2.8	5.17			
27	φ <sub>5</sub>	4.20	4.08	2.9	2.13	26.30	1.2	3.11			

<sup>a</sup> molecules cm<sup>-3</sup>. <sup>b</sup> × 100%. <sup>c</sup> Arbitrary units. <sup>d</sup> s<sup>-1</sup>. <sup>e</sup> molecules cm<sup>-3</sup> s<sup>-1</sup>. <sup>f</sup> Dimensionless. <sup>g</sup> Steady-state H-atom concentration calculated from the formula [H] = (k<sub>eHBr</sub>/k<sub>i</sub>)([HBr]<sub>0</sub>/[HBr] - 1) or [H] = ΔF<sub>HBr</sub>/k<sub>i</sub>[HBr].

Reaction occurs in a Teflon-coated cylindrical Pyrex reactor (V = 216 mL) mounted on a machined stainless-steel flange which contains an assembly allowing rapid interchange of exit orifice diameter between 0.2, 0.3, and 0.5 cm, denoted φ<sub>2</sub>, φ<sub>3</sub>, and φ<sub>5</sub>, respectively. The unimolecular escape rate constant is given by k<sub>eM</sub> = a<sub>φ</sub>(T/M)<sup>1/2</sup> s<sup>-1</sup>, where T is the absolute temperature, M is the mass of any individual gas component in the reaction cell, and a<sub>φ</sub> = 0.2785 for φ<sub>2</sub>, 0.5755 for φ<sub>3</sub>, and 1.352 for φ<sub>5</sub> orifices. The reaction cell temperature was held constant (±2 K) using a constant temperature bath circulator. Molecules exiting the cell are formed into a molecular beam in the differentially pumped system. The beam is modulated with a tuning fork chopper operated at 200 Hz prior to entering the ionizing field of a quadrupole mass spectrometer (Balzers QMG 511) fitted with a cross-beam analyzer. The ac component is filtered, amplified, and detected with a lock-in amplifier (ITHACO DYNATRAC 3 Model 393).

Signal intensities associated with species M, I<sub>M</sub>, at m/e 1 (H), 2 (H<sub>2</sub>), 36 and 38 (Ar), 79 and 81 (Br), 80 and 82 (HBr), and 158, 160, and 162 (Br<sub>2</sub>) were monitored under reactive and nonreactive conditions, with the ionization source operated at either 20 or 40 V. Two methods were employed to monitor and analyze the signal output from the lock-in amplifier. In initial experiments, the mass spectrometer was set to repeatedly scan a chosen mass (m/e) range, with signals recorded using a paper chart recorder (Houston Instrument 2000 Series X-Y

recorder). The height of each monitored peak was measured manually and then averaged to provide I<sub>M</sub>. In the second method, which superseded the first, the mass spectrometer was set to scan individual masses over a preset averaging period. The signal was then passed via a Keithley STA-08PGA screw terminal board to a PC and digitized using a Keithley Metrabyte Model DAS-8PGA 8 channel analog board. A modified version of Metrabyte's utility software, provided with the latter, controlled signal monitoring. The digitized signal was exported into Lotus 1-2-3 for processing. Results obtained from the two methods were indistinguishable (Table 1).

Calibration curves were produced for individual species by monitoring signal intensity, I<sub>M</sub>, as a function of the specific flux, F<sub>M</sub>, according to the relationship

$$I_M = \alpha_M F_M \quad (1)$$

where α<sub>M</sub> is the mass spectral efficiency for mass M and F<sub>M</sub>/molecule cm<sup>-3</sup> s<sup>-1</sup> = flux/V. The steady-state concentration of species M in the reaction cell is related to the specific flux via

$$[M]/\text{molecules cm}^{-3} = F_M/k_{eM} \quad (2)$$

Under the instrumental conditions employed, α<sub>M</sub> values for each species were relatively constant during the course of the

experimental series, however, values were collected during each experiment and applied in calculations for that specific experiment. Average  $\alpha_M$  values were

$$\alpha_{\text{HBr}} = (1.0 \pm 0.2) \times 10^{-11} \text{ (20 V)}$$

$$\alpha_{\text{Br}_2} = (4.8 \pm 0.7) \times 10^{-11} \text{ (20 V)}$$

$$\alpha_{\text{H}_2} = (3.4 \pm 0.6) \times 10^{-12} \text{ (40 V)}$$

$\alpha_{\text{Br}}$  was assumed equivalent in magnitude to  $\alpha_{\text{HBr}}$ .<sup>9</sup> Detailed experimental results are reproduced in Table 1 and are discussed in detail in the next section.

## Results and Discussion

The study of the title reaction was observed, in preliminary experiments, to have a number of difficulties associated with it which required modifications both to the experimental equipment and procedure in order to establish stable, reproducible conditions under which to make quantitative measurements. Firstly, in the earliest experiments, the detected H-atom signal (*m/e* 1) was observed to exhibit significant intensity fluctuations ( $\pm 30$ – $40\%$ ) relative to the variations in other signals ( $\pm 5$ – $10\%$ ) over similar averaging periods. As indicated in the previous section, prior to microwave discharge through the flowing  $\text{H}_2/\text{Ar}$  mixture, the gas passed first through a resistive capillary and then through the microwave tube. A flexible metal joint connected the two in order to allow rapid removal of the discharge tube for coating. Removal of this flexible joint, together with the insertion of a small length of capillary tubing ( $0.1 \text{ cm} \times 2 \text{ cm}$ ) just prior to the microwave tube produced a stable ( $\pm 5$ – $10\%$ ) H-atom signal, extraneous loss of H-atoms on the metal surface, and/or some back-diffusion out of the microwave region being minimized. Secondly, very small amounts of molecular bromine were detected in preliminary experiments. Background mass scans of the  $\text{HBr}/\text{Ar}$  mixtures indicated that the  $\text{Br}_2$  was not introduced as an impurity in the  $\text{HBr}$  flow. The small but detectable  $\text{Br}_2$  signal ( $< 2\%$  relative to  $[\text{HBr}]_{\text{ss}}$ ) was observed to decrease as a function of increasing microwave power. Operating above 35 W reduced the  $\text{Br}_2$  signal below the detection limits of our apparatus. This would appear in agreement with the earlier study of Heneghan and Benson<sup>10</sup> who found that microwave powers above 30 W dissociated upwards of 98% of  $\text{Br}_2$  in flowing  $\text{Br}_2/\text{He}$  mixtures.  $\text{Br}_2$  formation, in the present experiments, was suspected to occur following discharge of small amounts of  $\text{HBr}$  which were able to diffuse into the microwave discharge tube. At low microwave power, the volume of discharge tube the discharge itself "occupies" is small, allowing any  $\text{Br}_2$  formed to escape the tube and be detected subsequently. At higher microwave power, the discharge "occupies" a larger proportion of the discharge tube volume and any  $\text{Br}_2$  formed would be rapidly dissociated and hence not survive the discharge tube to be detected. Increased microwave power, along with the dimensions of the discharge zone, also increased the dissociative effect on any  $\text{Br}_2$  formed. Thirdly, H atoms and molecular  $\text{H}_2$  were produced from the phosphoric acid coating on the internal surfaces of the discharge tube. This effect occurred when either pure argon or experimental  $\text{H}_2/\text{Ar}$  mixtures were flowed through the tube under discharge conditions. Molina *et al.*<sup>11</sup> reported a similar effect with argon in a high pressure microwave system.

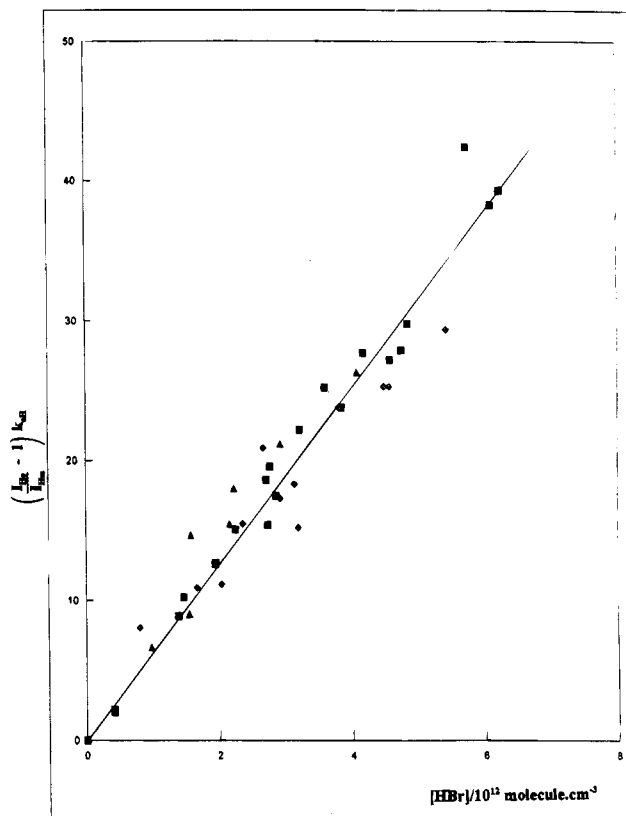


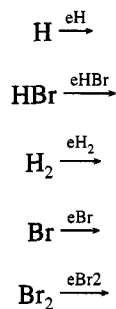
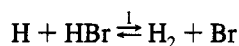
**Figure 1.** Plot of  $(I_{\text{H}0}/I_{\text{Hss}} - 1)k_{\text{eH}}$  vs  $[\text{HBr}]_{\text{ss}}$  at 298 K.  $[\text{HBr}]_{\text{ss}}$  in molecules  $\text{cm}^{-3}$ . ■,  $\phi_2$  ◆,  $\phi_3$  ▲,  $\phi_5$ .

There is a special problem involved in establishing mass balances between H or  $\text{H}_2$  and other much heavier gases such as  $\text{HBr}$  and  $\text{Br}_2$ . Mass balances at steady state require that  $|\Delta F_{\text{H}}| = |\Delta F_{\text{H}_2}| = |\Delta F_{\text{HBr}}| = |\Delta F_{\text{Br}}|$ . However, the relation between specific flux,  $F_M$ , and concentrations (eq 2) shows that these relations lead to the following relations in concentration:

$$\Delta[\text{H}]k_{\text{eH}} = |\Delta[\text{H}_2]|k_{\text{eH}_2} = |\Delta[\text{HBr}]|k_{\text{eHBr}} = \Delta[\text{Br}]k_{\text{eBr}} \quad (3)$$

For any given orifices, the escape constants vary inversely as  $M^{1/2}$  so that  $k_{\text{eH}} \approx 1.41k_{\text{eH}_2} \approx 9k_{\text{eHBr}} \approx 9k_{\text{eBr}}$ . Thus for a 50% increase in  $[\text{Br}]$ , there will only be a 5.5% decrease in  $[\text{H}]$  and about an 8% increase in  $\text{H}_2$ . A 50% decrease in  $[\text{H}]$  is accompanied by a 450% decrease in  $[\text{HBr}]$ . Because of this large disparity in relative concentration changes, small uncertainties in measurement of  $[\text{HBr}]$  signal are magnified almost 9-fold in the corresponding  $\Delta[\text{H}]$  signal. So long, however, as we allow sufficiently large changes in  $[\text{HBr}]$  to occur this does not interfere with the measurements of the rate constant (Figure 1). This effect reduced our ability to obtain mass balances for  $\text{H}_2$ , the latter always present in excess relative to  $\text{HBr}$  consumed in the reaction. From a steady-state analysis of the system, it can be shown that  $|\Delta F_{\text{H}_2}| = |\Delta F_{\text{HBr}}|$ . This relationship could not, however, be established in the present series of experiments (Table 1). With this effect noted, the present work relied on monitoring the signal intensities for the reactants, H and  $\text{HBr}$ , and monitoring the mass balance for bromine ( $\text{Br}_2$ ,  $\text{Br}$ , and  $\text{HBr}$ ). In the case of H atoms, the experiment involved monitoring signal intensities in the absence and presence of  $\text{HBr}$ . In the latter case, the flow of  $\text{HBr}$  was varied. Signals at *m/e* 1, 2, 79, 80, 81, 82, 158, 160, and 162 were monitored. Background intensities and fragmentation for all signals were recorded and taken into account in calculating actual signal intensities.

Reactions considered to occur under VLPR conditions were, on the basis of the observed products



where  $e\text{H}$ ,  $e\text{HBr}$ ,  $e\text{H}_2$ ,  $e\text{Br}$ , and  $e\text{Br}_2$  signify rate constants for escape from the reaction cell of the species shown (units of  $\text{s}^{-1}$ ). Solving the steady-state equation for  $[\text{H}]$ ,

$$k_{e\text{H}}[\text{H}]_0 = k_1[\text{H}]_{\text{ss}}[\text{HBr}]_{\text{ss}} + k_{e\text{H}}[\text{H}]_{\text{ss}} \quad (4)$$

where  $[\text{H}]_0$  and  $[\text{H}]_{\text{ss}}$  are the steady-state H-atom concentrations in the absence and presence of HBr, respectively. Rearranging eq 4 leads to

$$k_{e\text{H}}\left(\frac{[\text{H}]_0}{[\text{H}]_{\text{ss}}} - 1\right) = k_1[\text{HBr}]_{\text{ss}} \quad (5)$$

which in turn can be equated to

$$k_{e\text{H}}\left(\frac{I_{\text{H}_0}}{I_{\text{H}}} - 1\right) = k_1[\text{HBr}]_{\text{ss}} \quad (6)$$

where  $I_{\text{H}_0}$  and  $I_{\text{H}_{\text{ss}}}$  are the mass spectroscopic intensities at mass 1 at steady state in the absence and presence of HBr, respectively. The steady-state concentration of HBr is determined via

$$F_{\text{HBr}}^{\text{ss}} = k_{e\text{HBr}}[\text{HBr}]_{\text{ss}} = (I_{\text{HBr}})_{\text{ss}}/\alpha_{\text{HBr}} \quad (7)$$

where  $\alpha_{\text{HBr}}$  is the mass spectral efficiency for HBr. The latter is obtained from the slope of calibration plots of  $I_{\text{HBr}}$  as a function of known HBr specific flux,  $F_{\text{HBr}}$ , in the absence of reaction. Steady-state concentrations of HBr are in turn determined from measurements of  $(I_{\text{HBr}})_{\text{ss}}$  intensities under reaction conditions using eq 7. The latter are reproduced in Table 1 (column 4) along with the percentage of HBr consumed during reaction.

A plot of  $k_{e\text{H}}(I_{\text{H}_0}/I_{\text{H}_{\text{ss}}} - 1)$  vs  $[\text{HBr}]_{\text{ss}}$  yields a straight line plot with intercept zero and slope equal to  $k_1$  (Figure 1). This plot yields a value of  $(6.3 \pm 0.8) \times 10^{-12} \text{ cm}^3 \text{ molecule}^{-1} \text{ s}^{-1}$  under the established conditions at  $298 \pm 2 \text{ K}$ . In accord with eq 6, an intercept of  $0 \pm 5\%$  was experimentally determined. The latter is a well-defined datum using the present experimental analysis. With no HBr flowing into the reactor, i.e.,  $[\text{HBr}]_{\text{ss}} = 0$ , measurements of  $I_{\text{H}_0}$  and  $I_{\text{H}_{\text{ss}}}$  differ from each other only by random fluctuations in averaged signal intensity over the preset averaging period,  $I_{\text{H}_{\text{ss}}}$  in the absence of HBr being simply a second  $I_{\text{H}_0}$  measurement.

Data from the three orifices ( $\phi_2$ ,  $\phi_3$ , and  $\phi_5$ ), plotted on the same graph, are well represented by a single line indicating that the rate constant is essentially independent of variations in reactor residence time. The observed independence of  $k_1$  to variations in residence time, and in turn concomitant variations in the number of gas-wall collisions occurring, also indicate

that the reported results are not subject to any significant surface contribution. Experimental data from both chart recorder and computer averaging methods are included and show no distinguishable differences. A similar experimental procedure and analysis at 268 and 333 K yielded rate constants for reaction 1 of  $(5.4 \pm 0.7) \times 10^{-12}$  and  $(6.8 \pm 0.4) \times 10^{-12} \text{ cm}^3 \text{ molecule}^{-1} \text{ s}^{-1}$ , respectively. It should be noted that the majority of experimental results at 298 K and at 268 and 333 K relied predominantly on directly monitoring only the H-atom and HBr signals, with only a limited number of experiments involving simultaneous monitoring of reactants and products. Knowledge of H-atom and HBr signal intensities enabled values of  $k_1$  to be extracted *via* eq 6 as detailed. While only H-atom and HBr signal intensities were required to apply eq 6, absolute values for  $[\text{H}]_{\text{ss}}$  and  $[\text{H}]_0$  can be calculated using the  $k_1$  values determined from the data at each temperature *via*

$$[\text{H}]_{\text{ss}} = \frac{k_{e\text{HBr}}([\text{HBr}]_0 - 1)}{k_1} \quad (8)$$

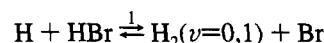
which is related to  $[\text{H}]_0$  *via*

$$[\text{H}]_0 = \left(\frac{I_{\text{H}_0}}{I_{\text{H}}}\right)[\text{H}]_{\text{ss}} \quad (9)$$

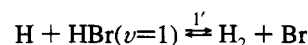
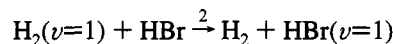
Values calculated for  $[\text{H}]_{\text{ss}}$  are reproduced in Table 1, column 8. In the final column of Table 1, the relationship  $I_{\text{Br}}/I_{\text{HBr}}$  reports bromine atom mass balance in terms of the recovery of bromine (Br, Br<sub>2</sub>, and HBr) exiting the reactor relative to the initial inflow of HBr. It should be noted that in runs 2 and 37, Br<sub>2</sub> was not specifically monitored and that in the latter run, a relatively low microwave discharge power (20 W) was also employed.

The rate constant for reaction 1 from the present study, at 298 K, compares favorably with the most recent measurements available in the literature (Table 2). Our value and those of Husain and Slater,<sup>3</sup> Jourdain *et al.*,<sup>4</sup> Umemoto *et al.*,<sup>5</sup> Seakins and Pilling,<sup>6</sup> and Talukdar *et al.*<sup>7</sup> are substantially higher than those of Glass and co-workers.<sup>1,2</sup>

As has previously been indicated,<sup>6</sup> reaction 1 is sufficiently exothermic to prepare H<sub>2</sub> in both ground and vibrationally excited states:



The formation of vibrationally excited H<sub>2</sub> in our steady-state VLPR system might conceivably lead to an apparent rate constant for reaction 1, enhanced relative to that which might be determined in a fully thermalized system. Vibrational energy transfer between H<sub>2</sub>( $\nu=1$ ) and HBr in reaction 2 leads to vibrationally excited HBr which can, in sufficient concentration, undergo reaction with H atoms, enhancing the measured value of  $k_1$ .



H atoms react much faster with HBr( $\nu=1$ ) than thermalized HBr and as a result the overall rate of consumption of HBr would be dependent upon the concentration of this excited species. Under steady-state conditions, the concentration of both H<sub>2</sub>( $\nu=1$ ) and HBr( $\nu=1$ ) are determined by their formation rates and also by homogeneous (gas-gas) and heterogeneous (gas-wall) quenching, together with their individual escape rates from the reactor. HBr( $\nu=1$ ) will also undergo spontaneous emission.<sup>9</sup>

**TABLE 2: Comparison of Literature Data for  $k_1$  with That from the Present Study**

method	$A/10^{-11} \text{ cm}^3 \text{ molecule}^{-1} \text{ s}^{-1}$	$(E/R)/\text{K}$	$k_1(298 \text{ K})/10^{-12} \text{ cm}^3 \text{ molecule}^{-1} \text{ s}^{-1}$	temp range/K	ref
DF-EPR <sup>a</sup>			$3.4 \pm 0.8$	298	1
DF-EPR	$27.7 \pm 3.2$	$1397 \pm 56$	$3.76 \pm 0.14$	230–318	2
FP-RF			$6.0 \pm 0.1$	298	3
DF-EPR			$6.3 \pm 0.5$	298	4
PR-RA	$2.5 \pm 0.7$	$397 \pm 72$	$6.3 \pm 0.4$	214–300	5
LP-RF	$1.87 \pm 0.3$	$310 \pm 50$	$6.54 \pm 0.66$	296–523	6
LP-RF	$2.96 \pm 0.44$	$460 \pm 40$	$6.47 \pm 0.55$	217–386	7
VLPR-MS			$6.3 \pm 0.8$	298	this work

<sup>a</sup> DF, discharge flow; EPR, electron paramagnetic resonance; FP, flash photolysis; RF, resonance fluorescence; PR, pulse radiolysis; RA, resonance absorption; LP, laser photolysis; VLPR-MS, very low pressure reactor coupled with mass spectrometry.

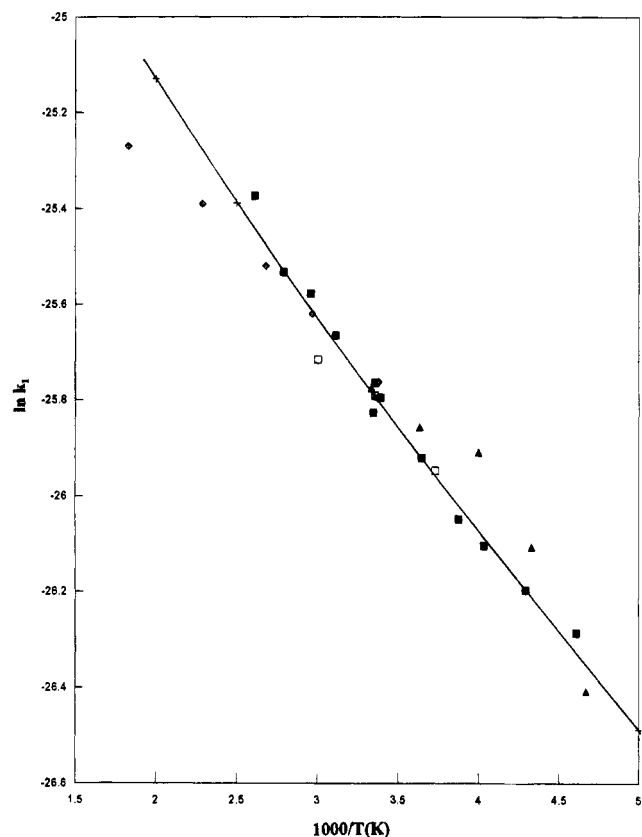


**Figure 2.** Arrhenius plot for reaction 1:  $\text{H} + \text{HBr} = \text{H}_2 + \text{Br}$ . ■, Talukdar *et al.*;<sup>7</sup> ◆, Seakins and Pilling;<sup>6</sup> ▲, Umemoto *et al.*;<sup>5</sup> □, this work.

Taking into account the likely production and loss rates for  $\text{HBr}$  ( $\nu=1$ ) the present authors estimate the latter's concentration to be less than 3–5% of the thermalized  $\text{HBr}$  concentration, suggesting a negligible effect on the value of  $k_1$  under the present experimental conditions. It should also be noted that experimental plots, which include kinetic data obtained from experiments conducted using three different orifices, exhibit excellent agreement. The variation in residence time and hence species escape rates allows a significant variation in both species concentration and in the number of homogeneous (gas–gas) and heterogeneous (gas–wall) collisions. It might be expected that if reaction 1' was a substantial contributor, data from the three orifices would not fall on the same kinetic line representing  $k_1$  (Figure 1). This was never found to be the case.

The temperature range of the present study, 268–333 K, was considered too limited on its own to yield an accurate Arrhenius expression for reaction 1. However, a preexponential factor,  $A_1/\text{cm}^3 \text{ molecule}^{-1} \text{ s}^{-1} = (2.8 \pm 0.6) \times 10^{-11}$  and  $E/R = (445 \pm 100) \text{ K}$  value (Figure 2) can be extracted by combining the present data with the extensive data of Talukdar *et al.*<sup>7</sup> Although  $k_1$  values at 298 K calculated from the Arrhenius parameters of

Umemoto *et al.*,<sup>5</sup> Seakins and Pilling,<sup>6</sup> and Talukdar *et al.*<sup>7</sup> are in good agreement with the value determined in the present study, the data of both Umemoto *et al.*<sup>5</sup> and Seakins and Pilling<sup>6</sup> appear to exhibit an unusual concavity in their temperature dependence, the former in the temperature range 214–300 K and the latter in the temperature range 296–546 K. Talukdar *et al.*<sup>7</sup> have previously discussed the agreement between their own data and that of Seakins and Pilling,<sup>6</sup> which exhibits a temperature range center of 421 K, significantly above the temperatures considered in the present study.

The present work, in combination with that of Talukdar *et al.*,<sup>7</sup> can be fitted to a modified Arrhenius expression,  $k_1/\text{cm}^3 \text{ molecule}^{-1} \text{ s}^{-1} = 9.96 \times 10^{-13} T^{0.5} \exp(-300/T)$ , and is suggested for use over the temperature range 200–1000 K. The  $T^n$  temperature dependence is in accord with that estimated using transition state theory (see next section). While somewhat different in form from the modified Arrhenius expression suggested by Seakins and Pilling,<sup>6</sup>  $k_1/\text{cm}^3 \text{ molecule}^{-1} \text{ s}^{-1} = 2.1 \times 10^{-14} T^{1.05} \exp(-82/T)$  over the range 214–1700 K,  $k_1$  values calculated from the two expressions, at the experimental temperatures reported by Seakins and Pilling<sup>6</sup> (296–546 K), differ by less than  $\pm 1.6\%$ . Differences in  $k_1$  values calculated from the two expressions between 200 and 1000 K differ by less than 17%, with the largest differences being exhibited at the temperature extremes.

### Transition State Calculation

An estimate of the preexponential factor for reaction 1 was made using transition state theory. The entropy of activation,  $\Delta S^\ddagger$ , for the reaction was calculated by applying the methods of Benson.<sup>12</sup> The reactant,  $\text{HBr}$ , was taken as a model for the transition state, and corrections were made to it in order to calculate the entropy of the actual assumed transition state  $[\text{H}\cdot\text{H}\cdot\text{Br}]^\ddagger$  and hence the entropy of activation for the overall reaction, where

$$\Delta S^\circ_{1^\ddagger} = (S^\circ_{\text{model}} - S^\circ_{\text{HBr}} - S^\circ_{\text{H}}) + \sum \Delta S^\circ(\text{corrections}) \quad (10)$$

and

$$\sum \Delta S^\circ(\text{corrections}) = \Delta S^\circ(\text{translational}) + \Delta S^\circ(\text{vibrational}) + \Delta S^\circ(\text{rotational}) + \Delta S^\circ(\text{electronic}) \quad (11)$$

Details of the correction terms, the equations, and structural parameters used in calculating them are reported in Tables 3 and 4. Preexponential factors of  $2.8 \times 10^{-11} \text{ cm}^3 \text{ molecules}^{-1} \text{ s}^{-1}$  and  $9.0 \times 10^{-11} \text{ cm}^3 \text{ molecules}^{-1} \text{ s}^{-1}$  were calculated for linear and bent transition state models, respectively. The major difference in  $\Delta S^\circ_{1^\ddagger}$  calculated for the two models is in the three-dimensional external rotation of the bent transition state, compared with the two-dimensional rotation of the linear transition state. As transition state theory calculations normally

TABLE 3: Transition State Calculation for the H + HBr Reaction

	$\Delta_{298}S^{\ddagger}(\text{linear})$	$\Delta_{300}C_p^{\ddagger}$	$\Delta_{400}C_p^{\ddagger}$	$\Delta_{500}C_p^{\ddagger}$	$\Delta_{298}S^{\ddagger}(\text{bent})$
model reaction					
H + HBr = [HBr] <sup>‡</sup>	-27.42	-5.00	-5.00	-5.00	-27.42
translation	0.04				0.04
electronic	1.38				1.38
rotation	3.28				5.93 (45°)
vibration					
-(H-Br) <sub>2650</sub>	0.00	0.00	0.00	-0.06	0.00
+(H·Br) <sub>1855</sub> (RC)	0.00	0.00	0.00	0.00	0.00
+(H·H) <sub>3080</sub>	0.00	0.00	0.00	0.00	0.00
+(H·H·Br) <sub>700</sub>	0.31	0.84	1.20	1.43	0.31
+(H·H·Br) <sub>700</sub>	0.31	0.84	1.20	1.43	
totals	-22.10	-3.32	-2.60	-2.20	-19.76

	$A \text{ (cm}^3 \text{ molecule}^{-1} \text{ s}^{-1}) = (e^2 kT/Nh)(R'T) \exp(\Delta S^{\ddagger}/R) = 10^{-5.73} \exp(\Delta S^{\ddagger}/R)$
correction formula	$\Delta S^{\circ}(\text{translation}) = \frac{3}{2}R \ln(M^{\ddagger}/M_{\text{model}})$ $\Delta S^{\circ}(\text{electronic}) = R \ln[(2S + 1)^{\ddagger}/(2S + 1)_{\text{model}}]$ $\Delta S^{\circ}(\text{vibration}) = -S^{\circ}(\text{vib})_{\text{model}} + S^{\ddagger}(\text{vib})$
linear model	$\Delta S^{\circ}(\text{rotation}) = S^{\ddagger}(2\text{-dimension}) - S_{\text{model}}(2\text{-dimension})$ $= R \ln(I^{\ddagger}\sigma_{\text{model}}/I_{\text{model}}\sigma^{\ddagger})$
bent model	$\Delta S^{\circ}(\text{rotation}) = S^{\ddagger}(3\text{-dimension}) - S_{\text{model}}(2\text{-dimension})$ $= [11.59 + (R/2) \ln[(I_a^{\ddagger}I_b^{\ddagger}I_c^{\ddagger})/\sigma^{\ddagger 2}] + 3R/2 \ln(T/298)] - [6.97 + R \ln(I_{\text{model}}/\sigma_{\text{model}}) + R \ln(T/298)]$

TABLE 4: Structural, Vibrational, and Rotational Parameters

property	H	HBr	H. H. Br
mass	1.008	80.912	81.92
bond distance (Å)			
H-Br		1.41	1.71
H-H			1.04
vibrations (cm <sup>-1</sup> )		2650	see above
moment of inertia (amu Å <sup>2</sup> )			
linear TS		1.979	10.324 <sup>a</sup>
		1.979	10.324
		0.0	0.0
bent TS		1.979	9.300
(H·H·Br) 45°		1.979	9.128
		0.0	0.172

<sup>a</sup> Principal moments of inertia for the transition states were calculated using GEOM, part of the UNIMOL package.<sup>13</sup>

predict preexponential factors to around a factor of 2 or better, the estimated preexponential factor for an assumed collinear transition state would appear in favorable agreement with the value of  $(2.8 \pm 0.6) \times 10^{-11} \text{ cm}^3 \text{ molecules}^{-1} \text{ s}^{-1}$  obtained by combination of the present data with that of Talukdar *et al.*<sup>7</sup> and also with the independent experimental determinations:  $(2.5 \pm 0.7) \times 10^{-11} \text{ cm}^3 \text{ molecules}^{-1} \text{ s}^{-1}$ ,<sup>5</sup>  $(1.87 \pm 0.3) \times 10^{-11} \text{ cm}^3 \text{ molecules}^{-1} \text{ s}^{-1}$ ,<sup>6</sup> and  $(2.96 \pm 0.44) \times 10^{-11} \text{ cm}^3 \text{ molecules}^{-1} \text{ s}^{-1}$ .<sup>7</sup> The estimated preexponential factor is also in excellent agreement with the much more computationally intensive theoretical calculations of Lynch *et al.*<sup>14</sup>

Calculated and experimentally determined preexponential factors<sup>5-7</sup> are an order of magnitude lower than the value reported by Endo and Glass,<sup>2</sup> suggesting that the latter's preexponential factor is unrealistically large. As indicated previously, the transition state calculation is unlikely to underestimate the actual preexponential factor by a full order of magnitude. Similarly, it is clear from the magnitude of the estimated preexponential factor,  $2.8 \times 10^{-11} \text{ cm}^3 \text{ molecule}^{-1} \text{ s}^{-1}$ , in combination with the reported rate constant,  $6.3 \times 10^{-12} \text{ cm}^3 \text{ molecule}^{-1} \text{ s}^{-1}$ , that reaction 1 exhibits a small, positive activation energy of the order of 0.5–1.0 kcal·mol<sup>-1</sup>. This would again suggest that the activation energy reported by Endo and Glass<sup>2</sup> is similarly too large. The uncertainties associated with the studies of Glass and co-workers<sup>1,2</sup> have been discussed at length elsewhere<sup>4,7</sup> and are not repeated here.

It is known<sup>12</sup> that the simple two-parameter form of the Arrhenius equation used to fit experimental temperature-

dependent data,  $k(\text{simple}) = A \exp(-E_{\text{act}}/RT)$ , can be related to the modified Arrhenius form,  $k(\text{modified}) = A'T^n \exp(-E'/RT)$  at  $T_m$ , the mean experimental temperature where, and only where,  $k(\text{simple}) = k(\text{modified})$ . Applying transition state theory, it can be shown that

$$k_1/\text{cm}^3 \text{ molecule}^{-1} \text{ s}^{-1} = \frac{e^2 k R' T_m^2}{h(N/10^3)} \left(\frac{T_m}{T_0}\right)^{\langle \Delta C_p^{\ddagger} \rangle / R} \times \exp\left(\frac{\Delta S^{\ddagger}}{R}\right) \exp(-E_{\text{act}}/RT_m) \quad (12)$$

which can be rearranged to

$$k_1/\text{cm}^3 \text{ molecule}^{-1} \text{ s}^{-1} = \frac{e^2 k R'}{h(N/10^3)} T_0^{-\langle \Delta C_p^{\ddagger} \rangle / R} \times \exp\left(\frac{\Delta S^{\ddagger}}{R}\right) T_m^{2+\langle \Delta C_p^{\ddagger} \rangle / R} \exp(-E_{\text{act}}^{\ddagger}/RT_m) \quad (13)$$

where  $k$  is the Boltzmann constant,  $R'$  is the gas constant in L atm mol<sup>-1</sup> K<sup>-1</sup>,  $h$  is Planck's constant,  $N$  is Avogadro's number, and  $\langle \Delta C_p^{\ddagger} \rangle$  is the average heat capacity of activation. Using a temperature range between 300 and 500 K for the calculation,  $\langle \Delta C_p^{\ddagger} \rangle / R = -1.48$  (Table 3). This suggests a  $T^{1/2}$  temperature dependence for reaction 1. At  $T_m = 400$  K, this translates into a preexponential factor of  $3.2 \times 10^{-11} \text{ cm}^3 \text{ molecule}^{-1} \text{ s}^{-1}$ , around a 15% increase in the value estimated at 298 K.

## Conclusions

Despite some minor difficulties in conducting a study of reaction 1, the VLPR technique enabled extraction of rate constants at 268, 298, and 333 K. The present experimental data confirms recent literature data available for the title reaction. Transition state estimates of the preexponential factor for reaction 1 appear in good agreement with both experimental data and more computationally intensive theoretical calculations.

Excited state reactions of HBr( $v=1$ ) are estimated to produce no measurable effect on the observed rate constant for reaction 1, the kinetics being completely described by the thermal rate constant,  $k_1$ .

The present experimental and theoretical work, together with that previously available in the literature, indicates that the rate constant for reaction 1 is very well established. It also indicates that transition state theory, as applied in the present work, is an

extremely powerful tool for investigating reaction temperature dependence and for calculating  $T^n$  dependence for the modified Arrhenius expression.

The VLPR technique has, for the first time, been shown to be effective in the analysis of reactions involving H atoms and can thus be applied to the study of these reactions with some confidence. Measurement of  $k_1$  under VLPR conditions allows reaction 1 to be employed as a method for calibrating absolute H-atom concentrations in future VLPR studies.

**Acknowledgment.** The authors thank Dr. Panos Papagianakopoulos for his assistance with the VLPR computer interface.

#### References and Notes

- (1) Takacs, G. A.; Glass, G. P. *J. Phys. Chem.* **1973**, *77*, 1060.
- (2) Endo, H.; Glass, G. P. *J. Phys. Chem.* **1976**, *80*, 1519.
- (3) Husain, D.; Slater, N. K. H. *J. Chem. Soc., Faraday Trans. 2* **1980**, *76*, 276.

- (4) Jourdain, J. L.; Le Bras, G.; Combourieu, J. *Chem. Phys. Lett.* **1981**, *78*, 483.
- (5) Umemoto, H.; Wada, Y.; Tsunashima, S.; Takayanagi, T.; Sato, S. *Chem. Phys.* **1990**, *143*, 333.
- (6) Seakins, P. W.; Pilling, M. J. *J. Phys. Chem.* **1991**, *95*, 9878.
- (7) Talukdar, R. K.; Warren, R. F.; Vaghijiani, G. L.; Ravishankara, A. R. *Int. J. Chem. Kinet.* **1992**, *24*, 973.
- (8) Dobis, O.; Benson, S. W. *Int. J. Chem. Kinet.* **1987**, *19*, 691.
- (9) Dobis, O.; Benson, S. W. *J. Phys. Chem.* **1995**, *99*, 4986.
- (10) Heneghan, S. P.; Benson, S. W. *Int. J. Chem. Kinet.* **1983**, *15*, 815.
- (11) Seeley, J. V.; Jayne, J. T.; Molina, M. J. *Int. J. Chem. Kinet.* **1993**, *25*, 571.
- (12) Benson, S. W. *Thermochemical Kinetics*, 2nd ed.; Wiley, New York, 1976.
- (13) Gilbert, R. G.; Smith, S. C.; Jordan, M. J. T. *UNIMOL: A program for calculation of rate coefficients for unimolecular and recombination reactions*; Department of Theoretical Chemistry, University of Sydney, Sydney, Australia, 1990.
- (14) Lynch, G. C.; Truhlar, D. G.; Brown, F. B.; Zhao, J.-G. *J. Phys. Chem.* **1995**, *99*, 207.

JP951701Z